Kidney Podocytes as Specific Targets for cyclo(RGDfC)-Modified Nanoparticles

*Klaus Pollinger, Robert Hennig, Miriam Breunig, Joerg Tessmar, Andreas Ohlmann, Ernst R. Tamm, Ralph Witzgall, and Achim Goepferich**

Renal nanoparticle passage opens the door for targeting new cells like podocytes, which constitute the exterior part of the renal filter. When cyclo(RGDfC)-modified Qdots are tested on isolated primary podocytes for selective binding to the αvβ3 integrin receptor a highly cell- and receptor-specific binding can be observed. In displacement experiments with free cyclo(RGDfC) IC_{50} values of 150 nM for αvβ3 integrin over-expressing U87-MG cells and 60 nM for podocytes are measured. Confocal microscopy shows a cellular Qdot uptake into vesicle-like structures. Our ex vivo study gives clear evidence that, after renal filtration, nanoparticles can be targeted to podocyte integrin receptors in the future. This could be a highly promising approach for future therapy and diagnostics of podocyte-associated diseases.

1. Introduction

The kidney and its interaction with nanoparticles play an increasingly important role in the field of nanomedicine. Recent publications have shown that intravenously administered nanoparticles can be cleared from the body by renal elimination.[1–5] This means that colloids like quantum dots (Qdots) can obviously have the ability to cross the renal filter, if they fulfill a plethora of physicochemical characteristics with regard to nanoparticle size, shape and charge.[1,6] Nanoparticles that overcome the renal barrier consequently could reach out for new targets since they pass certain cells like podocytes or tubular cells, which are otherwise out of reach for nanoparticles. With our study we intended to explore the possibility of a receptor-mediated nanoparticle delivery to the kidney.

Cells that would be highly attractive for a directed nanoparticle delivery as well as for drug delivery applications are podocytes. The reason lies in the fact that podocytes play a prominent role in kidney pathology. Various inherited diseases are associated with gene mutations in podocytes such as the nephritic syndrome,[7,8] nail-patella syndrome[9,10] or end stage renal disease.[11] But also acquired diseases like HIV-associated nephropathy,[12] diabetic nephropathy, focal segmental glomerular sclerosis and other acquired glomerular diseases can be traced to podocyte damage leading to severe kidney dysfunction.[13,14] Nanoparticle delivery to podocytes could, therefore, significantly increase therapeutic options in kidney therapy either as diagnostic tools or delivery vehicles for drugs and nucleic acids. To shed light on the feasibility of this approach, the present work investigates if a ligand-mediated interaction of nanoparticles with isolated podocytes and podocytes in whole glomeruli is possible and if these cells are able to incorporate such particles via receptor-mediated endocytosis.

For our studies we selected integrins as target receptors, since they are expressed in podocytes[15] and since they are known to be subject to high internalization rates,[16] which is important when it comes to the delivery of pharmaceutically active substances. Within the integrin family, the αvβ3 integrin

K. Pollinger, R. Hennig, Dr. M. Breunig,
Dr. J. Tessmar, Prof. A. Goepferich
Department of Pharmaceutical Technology
University of Regensburg
Universitätsstr. 31, 93053 Regensburg, Germany
E-mail: achim.goepferich@chemie.uni-regensburg.de
Prof. R. Witzgall
Institute for Molecular and Cellular Anatomy
University of Regensburg
Universitätsstr. 31, 93053 Regensburg, Germany
Dr. A. Ohlmann, Prof. E. R. Tamm
Institute for Human Anatomy and Embryology
University of Regensburg
Universitätsstr. 31, 93053 Regensburg, Germany

DOI: 10.1002/smll.201200733

small NANO MICRO

is supposed to be highly potent for a ligand-mediated nanoparticle delivery to cells, a receptor that even viruses make use of for their uptake into their target cells.[17] Furthermore, the $\alpha v\beta 3$ integrin is discussed to play a role in kidney pathology.[18,19] For the present work cyclo-(Arg-Gly-Asp-D-Phe-Cys) (cyclo(RGDfC)) was used as $\alpha v\beta 3$ specific ligand[20] and immobilized on Qdots, as model colloids, by covalent linkage. The Qdots used in this study carry a polyethylene glycol (PEG) coating, which suppresses non-specific binding to cells,[21] but also increases the hydrodynamic diameter and might therefore reduce or hinder their passage through the renal filtration barrier.[1] However, Qdots are ideal model nanoparticles for this study, since they can be easily detected due to their bright fluorescence in cellular binding studies.[22]

In the present study we addressed the key question, if a receptor-specific interaction of nanoparticles with podocytes is basically possible. Herein, the demand is to gain detailed insight to which extent nanoparticles bind to podocytes and to figure out the fate of nanoparticles after receptor binding. To obtain such a close insight into podocyte-material interaction we carried out an ex vivo analysis on podocytes and whole glomeruli. Such detailed studies with primary cells are of paramount importance to further understand receptor-mediated interactions of nanomaterials within the body.

2. Results and Discussion

2.1. Cyclo(RGDfC) Modification of Qdots

Amine-functionalized Qdots were labeled with cyclo(RGDfC), an $\alpha v\beta 3$ integrin specific ligand, using sulfo-SMCC linker chemistry as summarized in **Figure 1**A. Transmission electron microscopy (TEM) (Figure 1B) gave evidence that the labeling

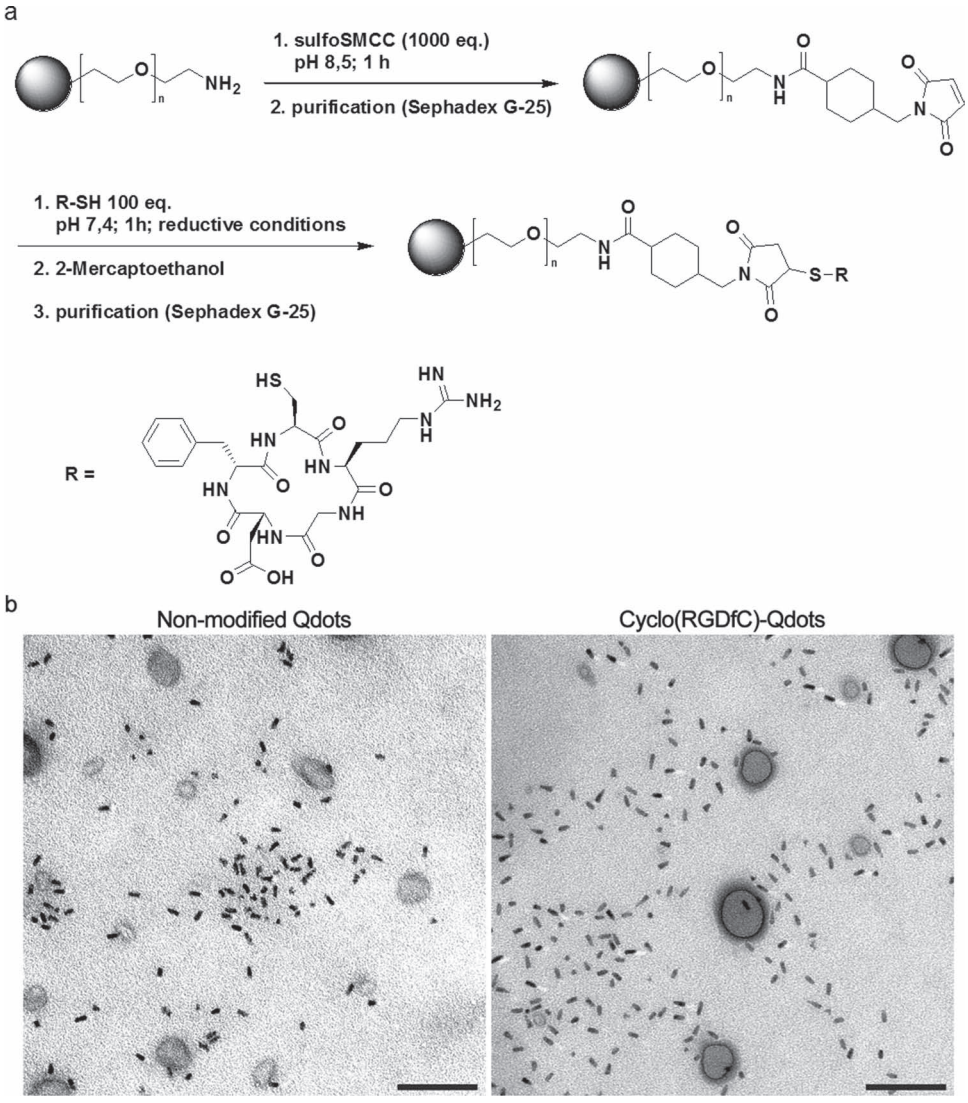

Figure 1. Qdots 655 with amine-terminated PEG coating as outer layer serve as starting material for covalently ligand modified Qdots. In the first step Qdots are activated for thiol reactivity with sulfo-SMCC, by amide formation. After purification by gel filtration chromatography, the maleimide carrying Qdots are incubated with cyclo(RGDfC) forming a thioether bond on the nanoparticle surface. Electron microscopy pictures showing Qdots before and after the labeling procedure reveal no changes in the nanoparticle appearance such as aggregation. The inorganic cores of the Qdots are rod-shaped with a length of 10 nm to 15 nm and a width of approximately 5 nm. (Magnification: 160,000, Scale bar: 100 nm)

procedure did not lead to a change of Qdots morphology. No aggregation tendency of nanoparticles after ligand modification was detectable, which guarantees a constant quality of Qdots and prevents non-specific cell interaction. TEM further revealed that the inorganic core of the Qdots was rod-shaped. To confirm the functionality of cyclo(RGDfC)-modified Qdots, they were tested on U87-MG cells as an $\alpha v\beta 3$ integrin positive cell line[23,24] and MCF-7 cells as negative control that do not express the $\alpha v\beta 3$ integrin.[25] For the present study, U87-MG cells are not only an ideal positive control. They can rather serve as an ideal benchmark for nanoparticle binding in comparison to primary cells, as they highly over-express the $\alpha v\beta 3$ integrin.[26,27]

Flow cytometry measurements (**Figure 2**A) showed that untreated cells only give a negligible autofluorescence, which does not affect the binding experiments with Qdots. Furthermore, both cell lines only exhibited a low interaction with non-targeted Qdots, indicating that non-specific binding only played a minor role. Incubation of $\alpha v\beta 3$ expressing U87-MG cells with cyclo(RGDfC)-Qdots revealed a strong binding to these cells. In contrast, the $\alpha v\beta 3$ integrin negative MCF-7 cells do not show an increased fluorescence after incubation with cyclo(RGDfC)-Qdots. These findings reveal that the cyclo(RGDfC)-Qdots exhibit a cell-selective binding, exclusively to $\alpha v\beta 3$ integrin expressing cells. Moreover, the strong interaction of cyclo(RGDfC)-Qdots is reflected by an almost ten-fold increase of cell-associated fluorescence compared to the non-specific binding of Qdots. In competitive displacement experiments it could be shown that a 1000-fold excess of free receptor ligand is needed to enforce a total loss of cell-associated fluorescence standing for a complete displacement of cyclo(RGDfC)-Qdots. The successful competitive displacement of peptide-modified Qdots verifies that this binding can be attributed to a specific receptor-ligand interaction among nanoparticles and cell surface receptors. Taking further into consideration that MCF-7 cells do not express the $\alpha v\beta 3$ but the related $\alpha v\beta 5$ integrin,[25] it can be concluded that nanoparticle binding is truly $\alpha v\beta 3$ integrin specific. This is highly desirable since the $\alpha v\beta 5$ integrin is found on a large number of cells in the body like macrophages or blood platelets, which would reduce the availability of nanoparticles to the target cells and could lead to unwanted side-effects on off-target cells.

These binding properties make cyclo(RGDfC)-modified Qdots ideal candidates for evaluating the receptor-mediated targeting potential of nanoparticles to kidney podocytes.

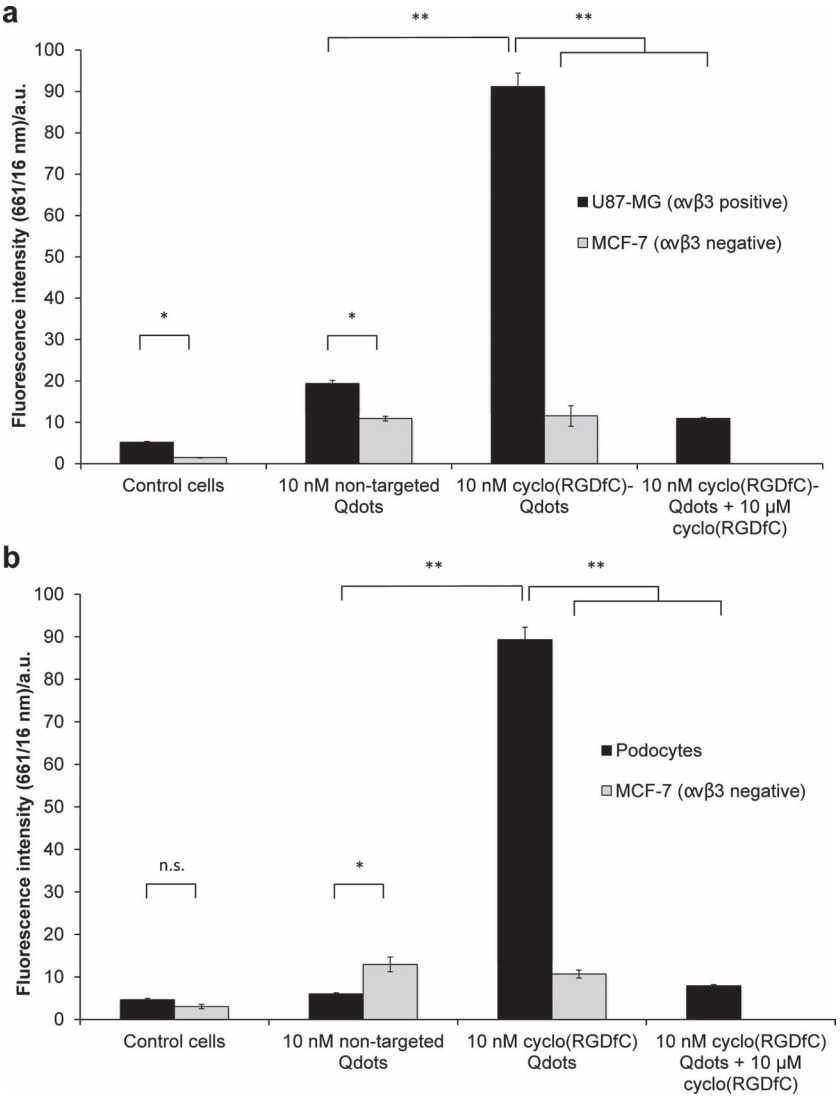

Figure 2. Flow cytometry based nanoparticle binding assay. (A) represents the comparison for receptor expressing U87-MG and off-target MCF-7 cells. Cyclo(RGDfC)-Qdots show a strong binding to U87-MG but no binding to MCF-7 cells. The displacement experiment with a surplus of free cRGDfC confirms the receptor-mediated nature of nanoparticle binding. The non-specific binding of unmodified Qdots is low for both cell lines. (B) represents the comparison for podocytes and MCF-7 cells. Here, flow cytometry experiments show a very pronounced binding of cyclo(RGDfC)-Qdots to podocytes, whereas only low non-specific binding of non-targeted Qdots can be detected. The receptor-mediated manner was verified by the displacement with a 1000-fold excess of free cyclo(RGDfC). Levels of statistical significance are indicated as $p < 0.05$ (*), $p < 0.01$ (**) and not significant (n.s.).

2.2. Nanoparticle Binding to Glomeruli

After cyclo(RGDfC)-modified Qdots had been successfully proven to bind to the $\alpha v\beta 3$ integrin receptors of U87-MG cells, we investigated the feasibility of receptor-mediated nanoparticle binding to glomerular podocytes in an ex vivo study. Herein the first aspect was, to investigate binding properties and distribution of Qdots in glomeruli. The advantage of using freshly prepared, whole glomeruli for nanoparticle binding studies is that podocytes are kept on their natural extra cellular matrix (ECM) substrate and their native environment. This procedure gives the best

small NANO MICRO

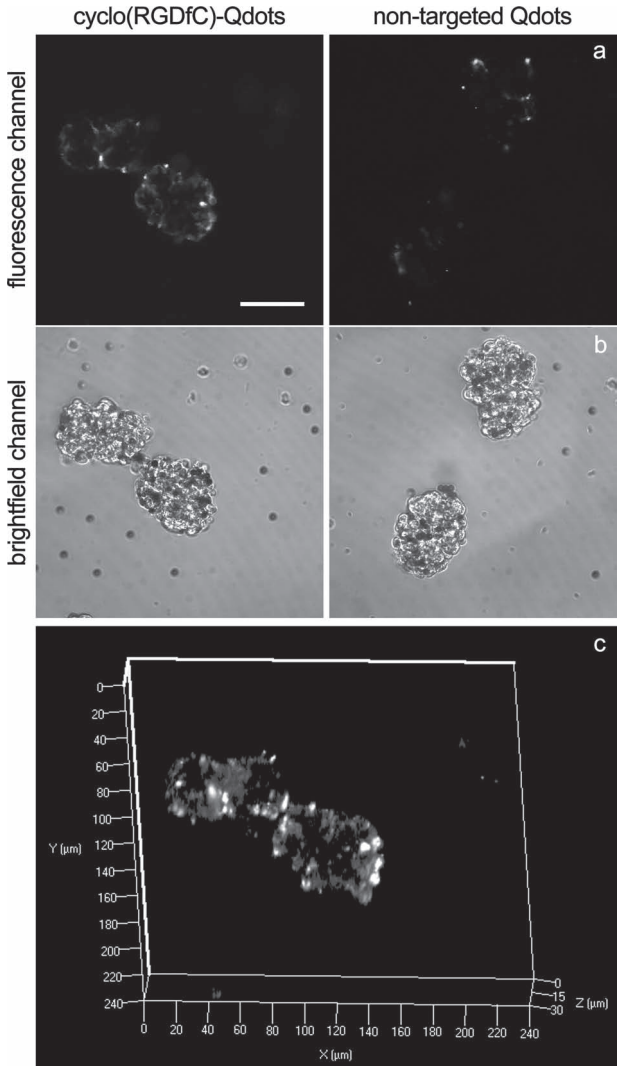

Figure 3. Confocal microscopy pictures showing glomeruli incubated with 30 nM cyclo(RGDfC)-Qdots or non-targeted Qdots. Scale bar 50 µm. The upper row (A) represents the fluorescence channel (confocal cross sections of 2 µm thickness) with Qdot fluorescence displayed in green. The lower row (B) shows the corresponding brightfield micrographs. Cyclo(RGDfC)-modified Qdots show a strong association with podocytes, located on top of the glomeruli, whereas non-targeted Qdots show no interaction. (C) shows a 3D image of Glomeruli incubated with 30 nM of cyclo(RGDfC)-Qdots. 15 confocal image slides of 2 µm thickness were stacked. The 3D picture illustrates the podocyte-associated distribution of cyclo(RGDfC)-Qdots on top of the glomeruli.

possible conservation of the native cell morphology and receptor expression.

CLSM was used to compare the binding properties of cyclo(RGDfC) decorated Qdots and non-modified Qdots (**Figure 3**A,B). A significant difference in glomeruli associated fluorescence intensity is obvious. Cyclo(RGDfC)-Qdots yielded a strong signal, whereas non-targeted Qdots stained the glomeruli only very weakly. This indicates that ligand modified Qdots had a high affinity to kidney glomeruli. Since the CLSM micrographs in Figure 3A and Figure 3B represent only 2 µm thick slices of whole glomeruli, a 3D picture was generated from a z-stack (Figure 3C) to investigate the fluorescence distribution over the whole glomerulus. The image reveals that the binding of cyclo(RGDfC) modified Qdots is highly pronounced in the exterior regions of glomeruli. This location of nanoparticle fluorescence on top of glomeruli corresponds precisely to the spots in which the podocyte cell bodies are located.

These findings show that a selective nanoparticle binding by podocytes residing in glomeruli is indeed feasible and that the $\alpha v\beta 3$ integrin seems to be an appropriate receptor to this end. Furthermore, it becomes evident that even though the receptor is involved in numerous bindings to natural ligands of the ECM, there is still enough $\alpha v\beta 3$ integrin available for binding cyclo(RGDfC)-Qdots.

2.3. $\alpha v\beta 3$ Integrin-Mediated Nanoparticle Targeting to Primary Podocytes

For a deeper understanding of cell-nanoparticle interactions, we quantified the binding behavior and the fate of cyclo(RGDfC)-Qdots after binding to primary podocytes.

The FACS measurements revealed a significant binding of cyclo(RGDfC)-modified Qdots to podocytes (Figure 2B). When comparing the binding of cyclo(RGDfC)-modified and non-targeted nanoparticles to podocytes, FACS data show a signal increase by a factor of almost ten. Receptor-negative MCF-7 cells showed no appreciable cyclo(RGDfC)-mediated nanoparticle binding, indicating a high selectivity of the peptide-modified Qdots to podocytes as target cells. The receptor-mediated nature of nanoparticle binding to primary podocytes was further proven by the fact that the cylo(RGDfC)-Qdots could also be displaced using an excess of free peptide. Furthermore, binding of non-targeted Qdots to podocytes was very weak, showing that non-specific binding effects are of minor significance and cell-nanoparticle interactions are mainly driven by receptor-ligand interactions.

These results show that cyclo(RGDfC)-modified nanoparticles do indeed hold a great potential for $\alpha v\beta 3$ integrin specific nanoparticle delivery. Even though the $\alpha v\beta 3$ integrin is not ubiquitous in the body its presence is discussed for a number of other kidney cells like epithelial- or endothelial cells.[28] Concomitantly it is described to be upregulated under pathological conditions in podocytes and mesangial cells for example.[19,29] Therefore, the binding affinity of cyclo(RGDfC)-Qdots to podocytes was investigated, which can have a major impact on target cell selectivity.

To quantify and compare the binding strength of $\alpha v\beta 3$ integrin targeted nanoparticles to podocytes and U87-MG cells, dose-response curves for the displacement of cyclo(RGDfC)-Qdots were determined (**Figure 4**). For both cell types characteristic sigmoidal displacement curves were obtained, which also reflects the receptor-mediated nature of nanoparticle binding to cells. The half-maximum displacement i.e. the IC_{50} values were 155 nM for U87-MG cells and 60 nM for podocytes.

From comparing the IC_{50} values of cyclo(RGDfC)-Qdots for both cell types it becomes obvious that the binding strength to podocytes only ranks shortly behind the cancer cell line. As U87-MG cells are known for their high $\alpha v\beta 3$

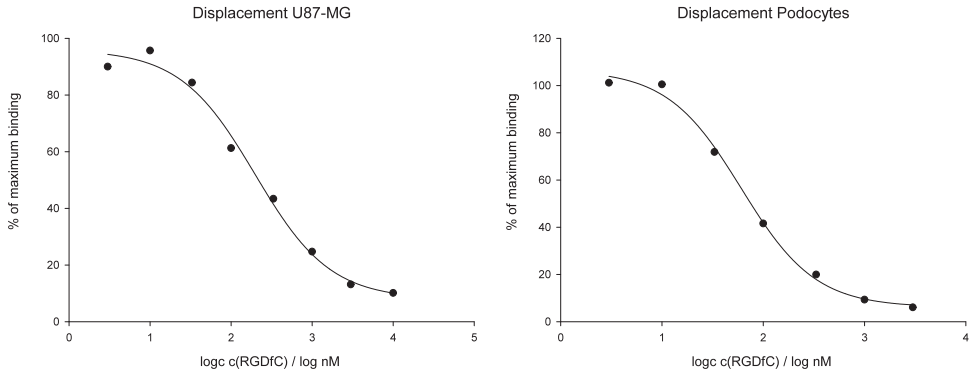

Figure 4. Displacement curves of cyclo(RGDfC)-Qdots for U87-MG cells and podocytes. A fixed amount of 10 nM cyclo(RGDfC)-Qdots was displaced using different concentrations of free cyclo(RGDfC) as competitor. IC_{50} values were determined to be 155 nM for U87-MG and 60 nM for podocytes. The results prove the receptor-mediated manner of Qdot binding to podocytes and show the high affinity of cyclo(RGDfC)-Qdots to both cell types.

integrin expression[23,24] and are used successfully for RGD-mediated tumor targeting strategies,[30] the high similarity in nanoparticle binding strength suggests that podocytes could be a similarly promising target cell.

2.4. Location of $\alpha v\beta 3$ Integrin Bound Nanoparticles

CLSM studies were performed to gain more insight into the location of cyclo(RGDfC) nanoparticles after binding to podocytes (**Figure 5**).

First of all it could be observed that the binding properties of the respective targeted and non-targeted nanoparticles strongly support the finding of a receptor-specific binding obtained by FACS analysis. The cyclo(RGDfC)-Qdots result in a strong cell-associated fluorescence, which can be displaced using a surplus of free cyclo(RGDfC). Non-targeted Qdots show a very weak binding to podocytes, which is due to unspecific cell binding. For the fluorescence of cyclo(RGDfC)-Qdots, a cellular distribution throughout the whole cytosol is found. This finding is supported by the fact that only the nuclei, located in the center of the cells, appear non-fluorescent in the CLSM micrographs. The intracellular distribution of Qdots is restricted to dotted structures in the whole cell bodies, indicating a localization of cyclo(RGDfC)-Qdots in vesicles. This distribution is most likely due to endocytotic

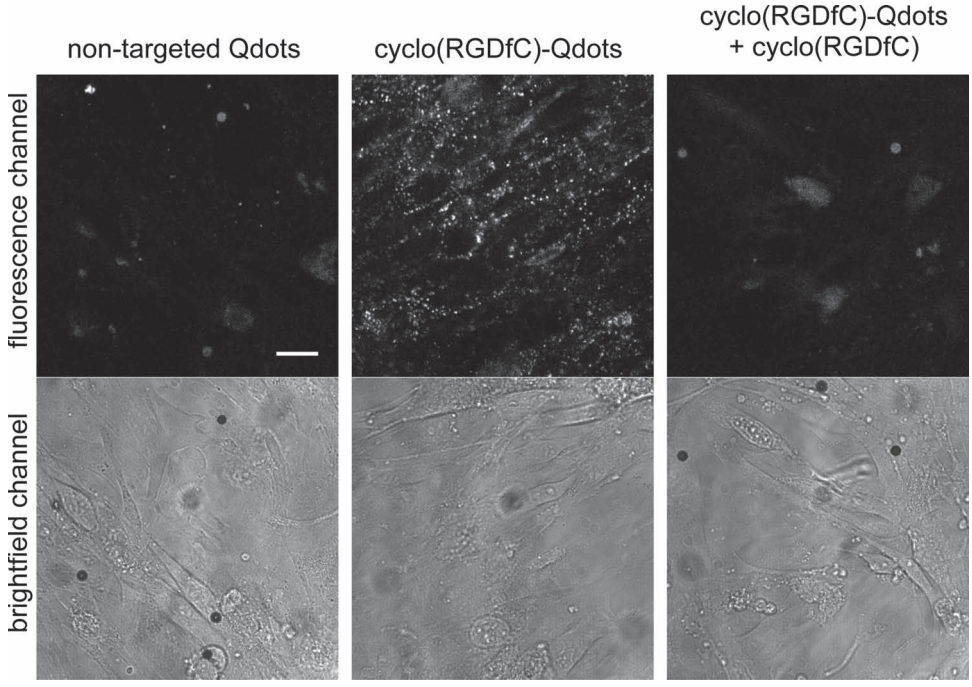

Figure 5. Confocal microscopy slides of 2D podocytes, incubated with 10 nM non-targeted or cyclo(RGDfC) modified Qdots, and displacement of 10 nM cyclo(RGDfC)-Qdots with 10 μM cyclo(RGDfC). The upper row shows the fluorescence channel (Qdot false color: green), the bottom row the corresponding bright-field channel. The receptor-mediated binding of cyclo(RGDfC)-Qdots was confirmed and the location of fluorescence indicated internalization of cyclo(RGDfC)-Qdots into podocytes. Scale bar: 20 μm.

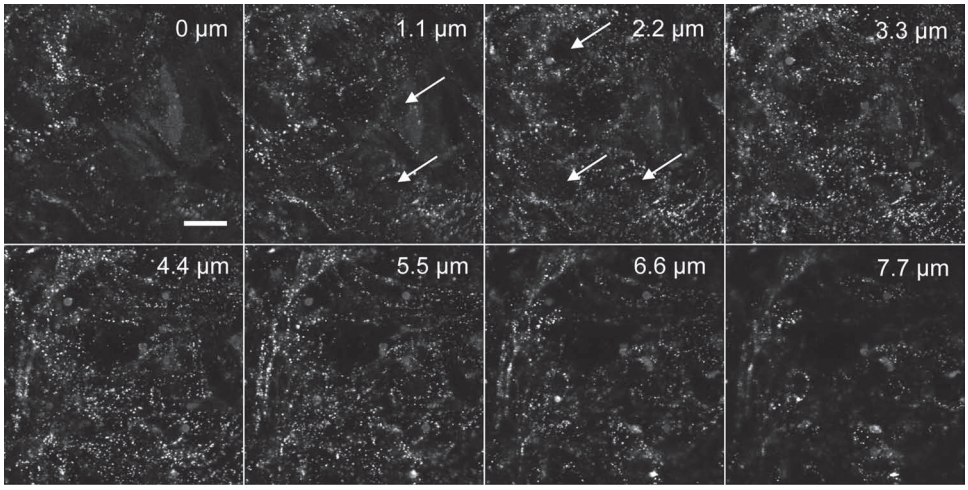

Figure 6. Confocal microscopy analysis of 2D-cultured podocytes, incubated with 10 nM cylco(RGDfC)-Qdots. The z-stack images show 1.1 µm thick slices of podocytes from the bottom to the top of the cells. Qdot-fluorescence is found throughout the cells, except for nuclei, in all layers from bottom to top. Exemplary nuclei are marked with white arrows. Scale bar: 20 µm.

uptake processes. Z-stack images (**Figure 6**) confirm that this fluorescence distribution is found throughout the cells.

In summary, the microscopic examination of 2D-cultured podocytes suggests that $\alpha v\beta 3$ integrin-mediated interaction with nanoparticles leads to an extensive nanoparticle uptake into the cells.

3. Conclusion

The present study strongly supports the hypothesis that kidney podocytes interact with receptor-addressed nanoparticles. In the future, the use of nanoparticles that are subject to effective renal filtration in combination with the presented strategy towards receptor-mediated targeting would mark an important step towards the development of new strategies for the therapy of podocyte-associated diseases. The presented results indicate that such a directed cell-material interaction is a highly promising approach in this field. Cyclo(RGDfC)-modified Qdots show a selective and receptor-mediated binding to podocytes in 2D cell culture and in whole glomeruli ex vivo. Furthermore, it was revealed that podocytes internalize these nanoparticles to a large extent into vesicular structures in the cytosol, which would be a prerequisite for intracellular therapeutic drug delivery. The renal filtration of nanoparticles is one of the most recent discoveries in current nanomaterial research. In future studies, the mechanism of nanoparticle passage through the renal filtration barriers has to be completely unraveled, as this will pave the way for specific nanoparticle delivery to podocytes.

4. Experimental Section

Materials: All chemicals were purchased from Sigma Aldrich (St. Louis, MO, USA) in analytical grade or higher if not stated differently. U87-MG glioblastoma cells and MCF-7 breast cancer cells were kindly provided by Prof. A. Buschauer (Faculty of Pharmacy and Chemistry, University of Regensburg). Buffers for peptide labeling of Qdots were borate buffer (10 mM $Na_2B_4O_7$, pH 8.5) and PBS (1.5 mM KH_2PO_4, 8 mM Na_2HPO_4, 2.7 mM KCl, 138 mM NaCl pH 7.4). Cell binding buffer was composed of 20 mM Tris, 150 mM NaCl, 2 mM $CaCl_2$, 1 mM $MnCl_2$, 1 mM $MgCl_2$ and 0.1% bovine serum albumin, pH 7.4.[31]

Nanoparticle Labeling (Figure 1): Qdots with a fluorescence emission of 655 nm, Qdot ITK amino (PEG) quantum dots (Molecular Probes, Eugene, OR, USA), served as raw material for the manufacture of cyclo(RGDfC)-modified nanoparticles. The nanocrystals consist of a CdSe core with a ZnS shell and carry an amphiphilic polymer coating, which provides water solubility of Qdots. To this polymer, amine-terminated polyethylene-glycol (PEG) is attached, which forms the outer layer of Qdots and allows for covalent surface modification. The thiol group of cyclo(RGDfC) was bound to the nanoparticle surface using sulfosuccinimidyl-4-(*N*-maleimidomethyl)cyclohexane-1-carboxylate (sulfo-SMCC) (Thermo Fisher, Waltham, MA, USA) as heterobifunctional linker. In the first step Qdots were activated for thiol reactivity with a 1000-fold molar excess sulfo-SMCC to the amount of Qdots in borate buffer pH 8.5 for 1 h. Subsequently, excess linker was removed by gel filtration chromatography (GFC) using a Sephadex G-25 resin in a PD-10 column (1.45 × 5.0 cm) (GE-Healthcare, Munich, Germany) and PBS pH 7.4 as elution buffer, resulting in pure maleimide activated Qdots. In the next step cyclo(RGDfC) was added in a 100-fold molar excess to the amount of nanoparticles and reacted for 1 h to form a thioether bond with the maleimides on the nanoparticle surface. Therefore, cyclo(RGDfC) was reduced in order to cleave disulfide bonds using tris(2-carboxyethyl)phosphine (TCEP), which was added to a solution of 0.4 mg/mL cyclo(RGDfC) at a concentration of 5 mM. After the reaction of Qdots with cyclo(RGDfC) the unreacted maleimide groups on the Qdot surface were inactivated using a 100-fold excess of 2-mercaptoethanol and reacted for another 30 min. Afterwards the reaction mixture was purified from the excess peptide and 2-mercaptoethanol by GFC as described above. For up-concentrating the Qdots, ultrafiltration was applied using a 100 kDa cut-off Amicon Ultra-4 filter unit (Milipore,

Billerica, MA, USA) for 10 min at 2000 g. Based on the work of Cai and coworkers, we estimated that approximately 90 RGD-peptides are bound per Qdot under these conditions.[32] The Qdot concentration was determined by fluorimetric measurement in 96-well plates on a LS-55 fluorescence spectrometer (Perkin Elmer, Waltham, MA, USA) using an excitation wavelength of 450 nm and an emission wavelength of 655 nm.[33]

Nanoparticles that are referred to as "non-targeted Qdots" were prepared as described above without cyclo(RGDfC). They served as control to assess the non-specific cell binding, since non-specific effects exhibited by the linker chemistry needed to be taken into account during the binding studies.

Transmission Electron Microscopy (TEM): Nanoparticle size was determined by electron microscopy. In doing so, a 2 μL droplet of a 10 nM nanoparticle solution was pipetted on a film coated copper grid (Plano, Wetzlar, Germany). The excess liquid was removed using a paper towel, resulting in a thin film of nanoparticle solution on the grid. After air-drying, Qdots were examined using a Zeiss Libra 120 electron microscope (Zeiss, Oberkochen, Germany). All pictures were recorded and analyzed with the Image SP software (Zeiss, Oberkochen, Germany).

Isolation of Glomeruli and Primary Podocytes: Glomeruli were isolated from the kidneys of female adult C57BL/6 mice on the basis of a publication by Takemoto and coworkers.[34] Mice were anaesthetized and the abdominal cavity and thorax were opened. A syringe, containing 40 mL of a magnetic bead suspension at a concentration of 2×10^6 beads/mL (Dynabeads, Invitrogen, Carlsbad, CA, USA), was inserted into the left ventricle and the abdominal aorta was cut open below the renal arteries. Subsequently, the magnetic bead suspension was injected at a constant pressure of 60 mm Hg. After perfusion, kidneys were removed from the body. Kidneys were decapsulated, cut into very small pieces (approx. 1 mm^3) using a scalpel and then digested for 30 min at 37 °C with 1 mg/mL of collagenase A (Roche Diagnostics, Penzberg, Germany). To remove larger pieces of tissue, the digested kidney was filtered using a 100 μm cell strainer (Becton-Dickinson, Franklin Lakes, NJ, USA) and the filtrate was washed extensively using a magnet to hold back glomeruli.

To obtain podocytes, glomeruli were plated in Dulbecco's Modified Eagle Medium (DMEM)/F-12 containing 10% fetal calf serum, 100 U penicillin/mL, 100 μg streptomycin/ml and insulin/transferrin/selenium-supplement (ITS) (PAA, Pasching, Austria) to allow for podocyte outgrowth to the bottom of a tissue culture flask for 5 days. After that podocytes were harvested by trypsinization and plated into 24-well plates or chambered cover slides at defined cell numbers for further experiments. For flow cytometry (FACS) experiments 50 000 cells per well were seeded into a 24-well plate. For confocal laser scanning microscopy (CLSM) 300 cells were seeded into chambered dishes with a cultivation area of 0.03 cm^2.

Cell Culture: The human neuronal glioblastoma cell line U87-MG was cultured in minimum essential medium containing Earl's salts (EMEM) (Sigma Aldrich, St. Louis, MO), supplemented with 10% fetal bovine serum (FBS) (Invitrogen, Carlsbad, CA, USA). Human breast cancer cell line MCF-7 was grown in EMEM with 5% FBS. Podocytes were cultured in DMEM/F-12 medium containing 10% fetal calf serum, supplemented with 100 U penicillin/mL, 100 μg streptomycin/ml and ITS (PAA, Pasching, Austria). Cells were cultured in T25 and T75 culture flasks (Corning, NY, USA). All cells were maintained in incubators at 37 °C with 5% CO_2 and 95% relative humidity.

Binding Studies Using Fluorescence Activated Cell Sorting (FACS): For binding studies cell-associated fluorescence was assayed by flow cytometry using a FACSCalibur flow cytometer (Becton Dickinson, Franklin Lakes, NJ, USA). In doing so, cells were seeded into 24-well plates (Corning, Corning, NY, USA) in the corresponding cell culture media. Seeding density of cells was 120,000 cells/well for U87-MG and MFC-7 cells and 50 000 cells/well for podocytes. After cultivation for 24 h, cells were incubated with differently grafted nanoparticles in cell binding buffer for 1 h at a concentration of 10 nM cyclo(RGDfC)-Qdots. To verify the receptor-mediated manner of nanoparticle binding, a competitive displacement experiment was carried out by adding a 1000-fold excess of free cyclo(RGDfC) as competitor. The non-specific cellular binding was investigated using 10 nM non-targeted Qdots. After cell incubation the culture medium containing Qdots was removed, the cells were washed with PBS and detached from the cell culture dish using an aqueous 0.25% trypsin solution. Subsequently cells were washed with ice cold PBS twice, dispersed in PBS and cell-associated fluorescence was analyzed by flow cytometry. Qdots were excited at 488 nm and fluorescence emission was detected using a 661/16 nm bandpass filter.

FACS data were analyzed using the WinMDI 2.9 software (The Scripps Research Institute, San Diego, CA, USA). The population of intact cells was gated and the geometrical mean of fluorescence intensity was determined. IC_{50} values were assessed by four-parameter sigmoidal fits using Sigmaplot 12.2 (Systat Software, Inc., San Jose, CA, USA).

Microscopic Nanoparticle Localization by Confocal Laser Scanning Microscopy: Cells were seeded in 8-well chamber slides (μ-slide 8 well, 1 cm^2 culture area, ibidi, Martinsried, Germany) or culture dishes with culture inserts (Culture-Insert StemCell, 0.03 cm^2 culture area, ibidi, Martinsried, Germany). After culturing the cells for 24 h in corresponding culture media, they were incubated with different nanoparticle species for 30 min. Before microscopy, cells were washed with PBS and supplemented with nanoparticle free incubation buffer.

Glomeruli were transferred into 8-well chamber slides directly upon isolation and incubated with nanoparticles without further culture. Here a concentration of 30 nM of Qdots was used and the incubation time was 2 h.

Whole glomeruli and podocytes were examined under a Zeiss Axiovert 200 microscope combined with a LSM 510 laser-scanning device using a 40× Plan-Neofluar (NA 1.3) objective for glomeruli and a 63 × Plan-Apochromat (NA 1.4) objective (Zeiss, Oberkochen, Germany) for cell monolayers. Qdots were excited with an Ar-laser at 488 nm and emission was detected using a 650 nm long-pass filter. Z-stacks were taken with a 1.1 μm step width for 2D cultured cells and 2 μm for glomeruli. For reasons of improved visibility Qdot fluorescence was displayed in false color green. The software used for image acquisition and processing was AIM 4.2 and ZEN 2008.

Statistics: One-way analysis of variances (ANOVA) was carried out combined with a multiple comparisons test (Tukey's test) to assess statistical significance. Levels of significance were set as indicated.

Acknowledgements

The authors thank Renate Liebl, Marion Kubitza and Margit Schimmel for excellent technical assistance in cell preparation and electron microscopy. This work was supported by the DFG (Deutsche Forschungsgemeinschaft) "graduate college GRK760" and by the DFG grant No GO565/17-1.

[1] H. S. Choi, W. Liu, P. Misra, E. Tanaka, J. P. Zimmer, B. Itty Ipe, M. G. Bawendi, J. V. Frangioni, *Nat. Biotechnol.* **2007**, *25*, 1165–1170.
[2] L. Lacerda, M. A. Herrero, K. Venner, A. Bianco, M. Prato, K. Kostarelos, *Small* **2008**, *4*, 1130–1132.
[3] H. S. Choi, B. I. Ipe, P. Misra, J. H. Lee, M. G. Bawendi, J. V. Frangioni, *Nano Lett.* **2009**, *9*, 2354–2359.
[4] C. Zhou, M. Long, Y. Qin, X. Sun, J. Zheng, *Angew. Chem. Int. Ed. Engl.* **2011**, *50*, 3168–3172.
[5] J. Gao, K. Chen, R. Luong, D. M. Bouley, H. Mao, T. Qiao, S. S. Gambhir, Z. Cheng, *Nano Lett.* **2012**, *12*, 281–286.
[6] A. Ruggiero, C. H. Villa, E. Bander, D. A. Rey, M. Bergkvist, C. A. Batt, K. Manova-Todorova, W. M. Deen, D. A. Scheinberg, M. R. McDevitt, *Proc. Natl. Acad. Sci. USA* **2010**, *27*, 12369–12374.
[7] N. Boute, O. Gribouval, S. Roselli, F. Benessy, H. Lee, A. Fuchshuber, K. Dahan, M. C. Gubler, P. Niaudet, C. Antignac, *Nat. Genet.* **2000**, *24*, 349–354.
[8] M. Kestilä, U. Lenkkeri, M. Männikkö, J. Lamerdin, P. McCready, H. Putaala, V. Ruotsalainen, T. Morita, M. Nissinen, R. Herva, C. E. Kashtan, L. Peltonen, C. Holmberg, A. Olsen, K. Tryggvason, *Mol. Cell* **1998**, *1*, 575–582.
[9] R. Witzgall, *Pediatr. Nephrol.* **2008**, *23*, 1017–1020.
[10] R. Morello, B. Lee, *Pediatr. Res.* **2002**, *51*, 551–558.
[11] B. Hinkes, R. C. Wiggins, R. Gbadegesin, C. N. Vlangos, D. Seelow, G. Nürnberg, P. Garg, R. Verma, H. Chaib, B. E. Hoskins, S. Ashraf, C. Becker, H. C. Hennies, M. Goyal, B. L. Wharram, A. D. Schachter, S. Mudumana, I. Drummond, D. Kerjaschki, R. Waldherr, A. Dietrich, F. Ozaltin, A. Bakkaloglu, R. Cleper, L. Basel-Vanagaite, M. Pohl, M. Griebel, A. N. Tsygin, A. Soylu, D. Müller, C. S. Sorli, T. D. Bunney, M. Katan, J. Liu, M. Attanasio, J. F. O'toole, K. Hasselbacher, B. Mucha, E. A. Otto, R. Airik, A. Kispert, G. G. Kelley, A. V. Smrcka, T. Gudermann, L. B. Holzman, P. Nürnberg, F. Hildebrandt, *Nat. Genet.* **2006**, *38*, 1397–1405.
[12] T.-C. Lu, J. C. He, P. E. Klotman, *Nephron Clin. Pract.* **2007**, *106*, c67–71.
[13] H. Cheng, R. C. Harris, *Int. J. Biochem. Cell Biol.* **2010**, *42*, 1380–1387.
[14] P. W. Mathieson, *Curr. Opin. Nephrol. Hypertens.* **2009**, *18*, 206–211.
[15] S. Schordan, E. Schordan, K. Endlich, N. Endlich, *Am. J. Physiol. Renal Physiol.* **2011**, *300*, F119–32.
[16] P. T. Caswell, S. Vadrevu, J. C. Norman, *Nat. Rev. Mol. Cell Biol.* **2009**, *10*, 843–853.
[17] T. J. Wickham, P. Mathias, D. A. Cheresh, G. R. Nemerow, *Cell* **1993**, *73*, 309–319.
[18] K. Amann, C. S. Haas, J. Schüssler, C. Daniel, A. Hartner, H. O. Schöcklmann, *Nephrol. Dial. Transplant.* **2012**, *27*, 1755–1768.
[19] A. Baraldi, G. Zambruno, L. Furci, M. Ballestri, A. Tombesi, D. Ottani, L. Lucchi, E. Lusvarghi, *Nephrol. Dial. Transplant.* **1995**, *10*, 1155–1161.
[20] M. Aumailley, M. Gurrath, G. Müller, J. Calvete, R. Timpl, H. Kessler, *FEBS Lett.* **1991**, *291*, 50–54.
[21] B. D. Chithrani, W. C. W. Chan, *Nano Lett.* **2007**, *7*, 1542–1550.
[22] T. Jamieson, R. Bakhshi, D. Petrova, R. Pocock, M. Imani, A. M. Seifalian, *Biomaterials* **2007**, *28*, 4717–4732.
[23] F. Li, J. Liu, G. S. Jas, J. Zhang, G. Qin, J. Xing, C. Cotes, H. Zhao, X. Wang, L. A. Diaz, Z.-Z. Shi, D. Y. Lee, K. C. P. Li, Z. Li, *Bioconjug. Chem.* **2010**, *21*, 270–278.
[24] Z.-B. Li, K. Chen, X. Chen, *Eur. J. Nucl. Med. Mol. Imaging* **2008**, *35*, 1100–1108.
[25] T. Meyer, J. F. Marshall, I. R. Hart, *Br. J. Cancer* **1998**, *77*, 530–536.
[26] X. Zhang, Z. Xiong, Y. Wu, W. Cai, J. R. Tseng, S. S. Gambhir, X. Chen, *J. Nucl. Med.* **2006**, *47*, 113–121.
[27] Z. Liu, B. Jia, H. Zhao, X. Chen, F. Wang, *Mol. Imaging. Biol.* **2011**, *13*, 112–120.
[28] H. Rabb, E. Barroso-Vicens, R. Adams, J. Pow-Sang, G. Ramirez, *Am. J. Nephrol.* **1996**, *16*, 402–208.
[29] E. G. Fischer, *Biochem. Cell Biol.* **2004**, *82*, 597–601.
[30] H.-Y. Lee, Z. Li, K. Chen, A. R. Hsu, C. Xu, J. Xie, S. Sun, X. Chen, *J. Nucl. Med.* **2008**, *49*, 1371–1379.
[31] W. Shi, J. S. Bartlett, *Mol. Ther.* **2003**, *7*, 515–525.
[32] W. Cai, K. Chen, Z.-B. Li, S. S. Gambhir, X. Chen, *J. Nucl. Med.* **2007**, *11*, 1862–1870.
[33] W. Cai, X. Chen, *Nat. Protoc.* **2008**, *3*, 89–96.
[34] M. Takemoto, N. Asker, H. Gerhardt, A. Lundkvist, B. R. Johansson, Y. Saito, C. Betsholtz, *Am. J. Pathol.* **2002**, *161*, 799–805.

Received: April 4, 2012
Revised: July 4, 2012
Published online: August 8, 2012

